

Thermodynamics and Mechanism of the Interaction of Willardiine Partial Agonists with a Glutamate Receptor: Implications for Drug Development

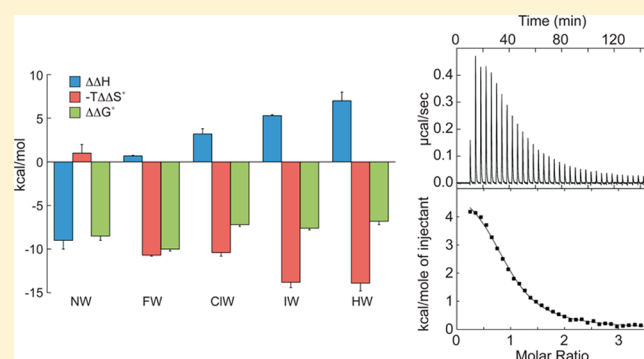
Madeline Martinez,[†] Ahmed H. Ahmed,[†] Adrienne P. Loh,[‡] and Robert E. Oswald^{*,†}

[†]Department of Molecular Medicine, Cornell University, Ithaca, New York 14853, United States

[‡]Department of Chemistry and Biochemistry, University of Wisconsin—La Crosse, La Crosse, Wisconsin 54601, United States

Supporting Information

ABSTRACT: Understanding the thermodynamics of binding of a lead compound to a receptor can provide valuable information for drug design. The binding of compounds, particularly partial agonists, to subtypes of the α -amino-3-hydroxy-5-methyl-4-isoxazole-propionic acid (AMPA) receptor is, in some cases, driven by increases in entropy. Using a series of partial agonists based on the structure of the natural product, willardiine, we show that the charged state of the ligand determines the enthalpic contribution to binding. Willardiines have uracil rings with pK_a values ranging from 5.5 to 10. The binding of the charged form is largely driven by enthalpy, while that of the uncharged form is largely driven by entropy. This is due at least in part to changes in the hydrogen bonding network within the binding site involving one water molecule. This work illustrates the importance of charge to the thermodynamics of binding of agonists and antagonists to AMPA receptors and provides clues for further drug discovery.



Understanding the thermodynamics of binding can be an important element in the optimization of the binding of a drug to its receptor.^{1–3} Ionotropic glutamate receptors are ligand-gated ion channels that are important drug targets because of their roles in a variety of neurological diseases, and in learning and memory.⁴ This group of neurotransmitter receptors consists of three major subtypes that include (1) α -amino-3-hydroxy-5-methyl-4-isoxazole-propionic acid receptors (AMPA; GluA1–4), (2) kainate receptors (GluK1–5), and (3) *N*-methyl-D-aspartic acid receptors (NMDA; GluN1, GluN2A–D, and GluN3A and -B). AMPA receptors are responsible for most of the fast excitatory transmission in the vertebrate central nervous system (CNS). They assemble as homo- or heterotetrameric channels, and each subunit is modularly arranged with an N-terminal domain, a ligand-binding domain (LBD), a transmembrane region, and a C-terminal domain.⁵ Both extracellular domains are arranged as dimers of dimers, with subunit crossover occurring between the N-terminal and ligand-binding domains.⁶ The LBD can be produced in isolation by bacterial expression⁷ and has been shown to be an effective model system for understanding the details of effector binding.⁸

The LBD is a bilobed structure, and glutamate binds in the cleft between the two lobes. The mechanism of activation follows a three-step process, which includes the binding of glutamate to lobe 1, followed by closure of the lobes and interaction with lobe 2, and finally the stabilization of the closed lobe form with the formation of two hydrogen bonds.⁹ A range

of compounds can bind to the agonist site, all of which bind in the same manner to lobe 1. The size of the compound, the characteristics of the interaction with lobe 2, and the stability of the fully closed form (including the presence of two stabilizing hydrogen bonds) determine if a compound is a full agonist, partial agonist, or antagonist. This is illustrated by derivatives of the natural product, willardiine, which has served as a scaffold for a range of glutamateric agonists and antagonists.^{10,11} Substituting the willardiine ring at position 3 with a carboxybenzyl or carboxyethyl substituent results in an antagonist with binding driven largely by a favorable enthalpic decrease.¹² Alternatively, 5-iodowillardiine (IW) is a partial agonist with binding driven largely by an entropy increase at physiological pH.¹² We describe here the thermodynamics of the binding of a series of willardiine partial agonists^{13,14} to the GluA2 LBD using isothermal titration calorimetry (ITC). These analogues, modified at position 5 (F, Cl, I, H, and NO₂), illustrate the effect of ligand charge on the entropic and enthalpic contributions to the Gibbs free energy of binding and suggest how the structure of the agonist can be modified to optimize the enthalpic component of binding.

Received: April 28, 2014

Revised: May 21, 2014

Published: May 21, 2014

METHODS

Protein Purification. The plasmid for the GluA2 ligand-binding domain, GluA2 LBD, was provided by E. Gouaux. It consists of residues N392–K506 and P632–S775 of the full rat GluA2-flop subunit with a “GT” linker connecting K506 and P632.¹⁵ The plasmid was transformed in the Origami B (DE3) *Escherichia coli* strain, and the GluA2 LBD was expressed and purified as described previously.¹⁶ Because of the necessity of obtaining accurate protein concentrations and the difficulties with standard methods for protein concentration, thiol quantitation was used (Thiol and Sulfide Quantitation Kit, Molecular Probes), based on a method described by Singh et al.^{17,18} In this assay, the thiols in the protein reduce a disulfide-inhibited derivative of papain, which releases the active enzyme in a stoichiometric manner. A chromogenic papain substrate is then used to measure the activity of the enzyme colorimetrically. As a standard, Ellman’s Reagent was used to determine the thiol concentration of L-cysteine standard solutions. Because the number of thiols in each protein molecule is known (four cysteines), we can determine the number of protein molecules within the protein sample. At the same time, we determined the absorbance at 280 nm of an identical protein aliquot, which allowed us to determine the extinction coefficient for our preparation of GluA2 LBD (58363 M⁻¹). The protein concentrations reflect the GluA2 LBD monomer. The dimerization constant for the GluA2 LBD is on the order of 6–40 mM,^{19,20} so that no significant concentration of dimer was present at the concentrations of protein used in these experiments.

Isothermal Titration Calorimetry (ITC). ITC experiments were conducted on a Microcal VP-ITC calorimeter at 10, 15, and 20 °C. Willardiine derivatives were obtained from Tocris and Abcam Biochemicals. The final protein concentration ranged from 8 to 40 μM. Titrations were conducted in the same buffer over a range of temperatures (5–20 °C) using a syringe speed of 300 rpm and a reference power of 10 μcal/s. Typical titration experiments consisted of 35 injections in which the individual injections were 6 μL (0.4 mM ligand) and were made every 240 s. The calibrated cell feedback signal (microcalories per second) was collected at 2 s intervals. The areas derived from the first injection were not used in the analysis. Experimental data were corrected for buffer mismatch by subtracting control titrations of the ligand solution into the ITC buffer (phosphate or cacodylate).

The thermograms were analyzed using the competitive binding approach described by Sigurskjold et al.,²¹ with the glutamate-bound state as the reference state. Data were fit using a K_a for the binding of glutamate of 1.0×10^6 M⁻¹. The binding stoichiometry (n), the apparent enthalpy of binding ($\Delta\Delta H$), and K_a were obtained by fitting. The value of n is the molar ratio of the ligand to the protein, and $\Delta\Delta H$ is expressed in kilocalories per mole of injectant. The values of n , K_a , and $\Delta\Delta H$ were used to compute $\Delta\Delta S^\circ$ and $\Delta\Delta G^\circ$ at the experimental temperature (T). Whenever possible, the binding reactions were conducted at multiple temperatures, so that the change in heat capacity ($\Delta\Delta C_p$) of the binding reaction could be determined.

Implications of Competition Binding for Thermodynamic Parameters. Because of the low stability of the apo state in combination with the difficulty of completely removing glutamate from the GluA2 LBD sample, more consistent results were obtained using competition experiments, that is, the

competition of a given ligand with glutamate. The ground state is, in this case, defined as the glutamate-bound state rather than the apo state. For a related AMPA receptor LBD (GluA4), Madden and collaborators²² were able to obtain thermodynamic parameters for the binding of glutamate to the apo state (ΔH values of -2.49 ± 0.03 and -4.21 ± 0.03 kcal/mol at 15 and 20 °C, respectively; $-T\Delta S^\circ$ values of -5.39 and -3.96 kcal/mol at 15 and 20 °C, respectively; ΔC_p of -171 cal mol⁻¹ K⁻¹). Despite the fact that the binding sites of all AMPA receptors are very similar,^{23–25} the thermodynamic parameters for GluA4 LBD cannot necessarily be compared directly to the quantities determined for the GluA2 LBD. However, referencing the glutamate-bound state of GluA2 at physiological pH does reveal the quantitative and qualitative differences between the thermodynamic parameters of the binding of willardiine ligands, as shown in Figure 1C. Likewise, in the calculation of $\Delta\Delta C_p$ (slope of $\Delta\Delta H$ vs temperature), the reference state is constant for each temperature (Figure 3). ΔC_p (heat capacity relative to the apo state) would be determined by the difference between $\Delta\Delta C_p$ and the ΔC_p for glutamate relative to the apo state.

The ionization state of glutamate can change at high and low pH, in that the pK_a of the γ -carboxyl of glutamate is approximately 4 and that of the α -amine is approximately 9.5. Nevertheless, the nuclear magnetic resonance (NMR) spectra of glutamate bound to GluA2 LBD at these pH values are only slightly changed,⁹ suggesting that neither the uncharged γ -carboxyl form nor the uncharged α -amine form of glutamate is likely to bind. Thus, the ΔG° for binding of glutamate to the apo state would be unchanged, and the effect of pH on the willardiine binding would be reflected in the competition thermograms.

Crystallography. Crystals were grown using the hanging drop technique at 4 °C. Each drop contained a 1:1 (v/v) ratio of protein solution to reservoir solution [16–18% PEG 8K, 0.1 M sodium cacodylate, and 0.1–0.15 M zinc acetate (pH 3.5)]. Data were collected at Cornell High Energy Synchrotron Source (CHESS) beamline A1 (wavelength of 0.987 Å, temperature of 100 K) using a Quantum-210 Area Detector Systems charge-coupled device detector. Data were indexed and scaled using HKL-3000.²⁶ Structures were determined with molecular replacement and refined with Phenix.²⁷ Model building was conducted with Coot version 0.7.²⁸

RESULTS

The apo form of the GluA2 LBD is difficult to prepare and is much less stable than ligand-bound forms, so the experiments described here were conducted as competition binding relative to the glutamate-bound form. For this reason, thermodynamic parameters are expressed with the glutamate-bound form as the reference state ($\Delta\Delta H$, $-T\Delta\Delta S^\circ$, and $\Delta\Delta C_p$). Panels A and B of Figure 1 show thermograms (pH 7.2 and 20 °C) of the displacement of glutamate by 5-nitrowillardiine (NW) and IW. The most striking difference is that the reaction is exothermic for NW and endothermic for IW. The thermograms for 5-chlorowillardiine (CIW), willardiine (HW), and 5-fluorowillardiine (FW) indicate endothermic processes (Figure S1 of the Supporting Information). The enthalpy change becomes progressively less favorable with decreasing electronegativity of the substituent [increasing $\Delta\Delta H$ (Figure 1C)], with only NW having a favorable $\Delta\Delta H$ (-9 ± 1 kcal/mol). Conversely, at 20 °C, the entropic component of the displacement ($-T\Delta\Delta S^\circ$) is favorable for all of the derivatives except NW.

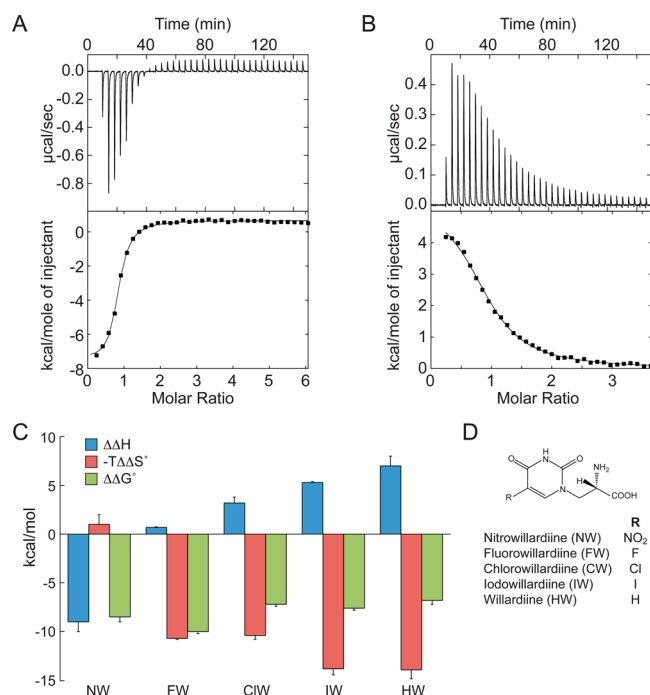


Figure 1. Thermograms showing raw (top) and integrated (bottom) data for NW (A) and IW (B) displacement of glutamate from the GluA2 LBD at 20 °C. The molar ratio is the ratio of ligand to protein. Fits were performed as described by Sigurskjold et al.²¹ (C) Calculated $\Delta\Delta H$, $-T\Delta\Delta S^\circ$, and $\Delta\Delta G^\circ$ values for displacement of glutamate by the five willardiine derivatives. (D) Structures of the willardiine derivatives.

The favorability of the entropy of binding decreases as a function of electronegativity, with IW and HW having the largest increases.

The influence of substituent electronegativity on the thermodynamic parameters suggested that the differing pK_a of the uracil ring, due to the different analogues in position 5, may affect the thermodynamics of binding. While the pK_a of all the halogenated uracils is ~ 8 , those of HW and NW are approximately 10 and 6, respectively.^{29,30} This means that willardiine and the halogenated analogues were, at physiological pH, in mostly uncharged (protonated) states (Figure 2A). NW, however, was in a mostly charged (deprotonated) state. The GluA2 LBD is well-behaved between pH 4 and 10, with minor changes in the NMR ^1H – ^{15}N HSQC spectrum.⁹ We tested the possibility that the charged state of the ligand could affect the enthalpy versus entropy distribution by changing the pH. Thus, binding of largely uncharged (protonated uracil ring) NW was examined at pH 4, and binding of largely charged (deprotonated uracil ring) HW was examined at pH 10.

Unlike the case at pH 7.2, at pH 10, the displacement of glutamate by HW (approximately 80% deprotonated) was exothermic, with a favorable binding enthalpy of -5 ± 1 kcal/mol (Figure 2B, 10 °C). The $\Delta\Delta H$ at pH 10 is 14 ± 3 kcal/mol more favorable than at pH 7.2. Deprotonation, however, results in a $-T\Delta\Delta S^\circ$ that is less favorable by 14 ± 3 kcal/mol than at pH 7.2. This is a clear example of enthalpy–entropy compensation, where the interactions that result in a favorable enthalpy change result in an increased order of the system, and thus in an equivalent entropic cost (decrease). The compensation between enthalpic and entropic factors results

in a negligible difference in $\Delta\Delta G^\circ$ between the binding of protonated and deprotonated forms of willardiine.

At pH 4, the uracil ring in NW is more than 97% protonated (uncharged). At this pH, the binding reaction is endothermic, unlike binding at pH 7.2, with a $\Delta\Delta H$ of 7 ± 1 kcal/mol (Figure 2B). This is 10 kcal/mol less favorable than the binding at pH 7.2. However, at pH 4, the $-T\Delta\Delta S^\circ$ is 7 ± 2 kcal/mol more favorable than in the deprotonated form. Although there is also an enthalpy–entropy compensation observed between the two pH values for NW, a decrease in the free energy of binding by 0.7 ± 0.3 kcal/mol is observed, with a lower binding affinity at pH 4. Because of the role of the side chain of E705 in the binding site (Figure 2C–E), the decrease in affinity at pH 4 could be, in part, related to a partial protonation at this site. Nevertheless, the data strongly indicate that, although pH is a minor determinant of $\Delta\Delta G^\circ$ (and, thus, the K_D of binding) of willardiine analogues, the distribution of entropy and enthalpy changes varies with the charged state of the uracil ring in a predictable way. In particular, a negatively charged state correlates with an exothermic binding enthalpy, while an uncharged state correlates with an endothermic binding enthalpy. This would suggest that for enthalpy optimization, the presence of a negative charge on the ligand as it interacts with lobe 2 would be preferred. This is consistent with the observed binding of other charged willardiines.¹²

The temperature profile of the thermodynamic parameters can provide more detailed insight into the binding modes of these ligands. Within a narrow temperature range, the temperature dependence of $\Delta\Delta H$ is given by

$$\Delta\Delta H = \Delta\Delta H_0 + \Delta\Delta C_p(T - T_0)$$

where $\Delta\Delta H_0$ is the binding enthalpy at an arbitrary reference temperature, T_0 , and $\Delta\Delta C_p$ is the heat capacity change of binding. The values of $\Delta\Delta C_p$ are determined from the slope of a plot of $\Delta\Delta H$ versus temperature as shown in Figure 3. The interpretation of $\Delta\Delta C_p$ is somewhat complex because it is based on a competition measurement. However, Madden and collaborators²² described the temperature dependence of ΔH for glutamate binding to the apo form in a related LBD (GluA4), and the $\Delta\Delta C_p$ was -171 cal mol⁻¹ K⁻¹. In comparison, the $\Delta\Delta C_p$ for NW binding relative to glutamate is more negative (-671 cal mol⁻¹ K⁻¹), suggesting that the ΔC_p for NW binding relative to that of the apo form would be considerably more negative than for glutamate binding. This is consistent with burying polar groups upon binding. In addition, in comparison to the other willardiine derivatives used, NW has a negatively charged nitro group at position 5 and, as discussed above, the uracil ring is largely charged at physiological pH. Thus, the uracil ring of NW is more charged than the other willardiines used or glutamate, consistent with its more negative change in heat capacity. For the other willardiines, which have largely uncharged uracil rings at physiological pH and have halogens or a proton at position 5, the temperature dependence of $\Delta\Delta H$ is similar to or less than that of glutamate alone, possibly suggesting that their ΔC_p (relative to apo) is either near zero or slightly negative. Given the polarity of the binding site and the H-bonds formed by the uracil ring with lobe 2 of GluA2, the binding is unlikely to be driven by the hydrophobic effect, which predicts a positive ΔC_p . Overall, because the binding of agonists and antagonists shows very consistent interactions with lobe 1, it is the interaction with lobe 2 that contributes to the thermodynamics of binding and the efficacy of a ligand. Like the pH effects described above, these results

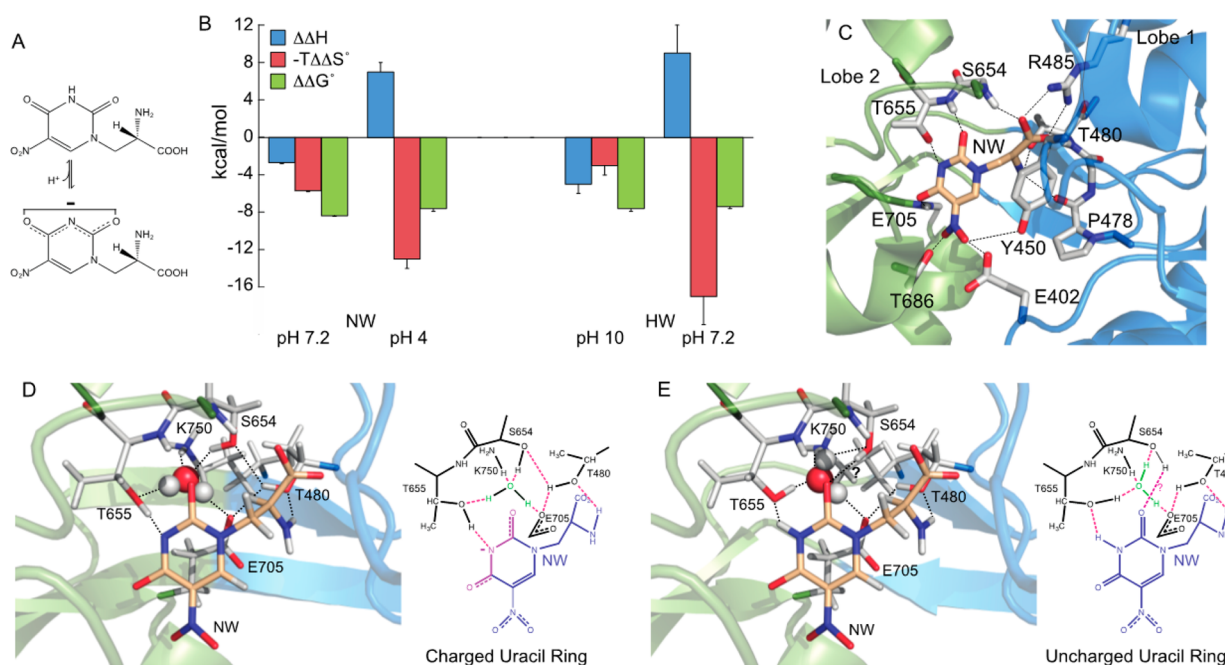


Figure 2. (A) Ionization states of the uracil ring of NW. Similar ionization states are possible for the other willardiine derivatives. (B) Effect of a change in pH on the thermodynamic parameters for NW (left) and HW (right) at 10 °C. For both compounds, the pH at which the ionized state is favored is shown on the left and that for which the un-ionized state is favored is shown on the right. (C) Structure of the binding site, showing the direct interactions between NW and the GluA2 LBD [Protein Data Bank (PDB) entry 3RTW³²]. (D) Structure of the binding site for NW showing the hydrogen bonding network associated with the nitrogen at position 3 of the willardiine ring in the charged form (pH 6.5, PDB entry 3RTW³²). On the left is the structure and on the right a schematic. In the schematic, NW is colored blue, the protein black, and water green and the H-bonds are colored red. (E) Structure of NW bound to the GluA2 LBD obtained at pH 3.5 (PDB entry 4Q30). At this pH, the ring is largely uncharged. The formatting of this panel is similar to that of panel D. Note the change in the H-bonding network. The potential H-bond between the hydroxyl of S654 and the uracil carbonyl is shown with a question mark because the distance between the two oxygens is relatively long, 3.5 Å, and the angle between this H-bond and the H-bond with the water is not favorable (80°).

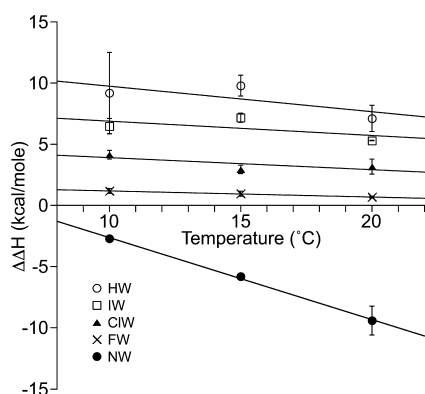


Figure 3. Dependence of $\Delta\Delta H$ on temperature.

suggest that charged interactions with lobe 2 contribute to the optimization of the enthalpy of the reaction, particularly at physiological temperatures (extrapolating from the temperature dependence shown in Figure 3).

While crystal structures of NW bound to GluA2 LBD differ little when the pH of the crystallization medium is changed from 6.5 (Figure 2D) to 3.5 (Figure 2E and Table S1 of the Supporting Information), the ITC results suggest that the binding interactions in the charged form differ significantly from those in the uncharged form. An extensive H-bonding network is present in which both the nitrogen at position 3 on the uracil ring and the α -amide are involved. A similar network is observed for all of the willardiine derivatives modified at position 5 and bound to GluA2^{14,31,32} or GluA3.³² A change in

the configuration of the H-bond donors and acceptors could accommodate the charged and uncharged forms of the uracil ring (Figure 2D vs Figure 2E), maintaining a similar network. In the charged form (Figure 2D), the H-bond between the willardiine and the hydroxyl of T655 may be stronger, perhaps giving rise to the more favorable enthalpy change. Additionally, the number of H-bonds formed by the hydroxyl of S654 is expected to change with the charge state. If the uracil ring is charged, the hydroxyl of S654 forms two favorable H-bonds. However, when the uracil ring is uncharged, the H-bond with water seems favorable, but the H-bond shown with the ring carbonyl does not have a favorable angle or distance and may or may not be present, possibly reducing the enthalpy of binding at lower pH values. Although this is a complex experiment because it compares bound willardiine to bound glutamate, the glutamate reference state remains largely constant (for a given condition). Thus, the binding of the charged state of the willardiines may be expected to have a change in enthalpy more favorable than that of the uncharged state. Interaction with solvent may also affect the thermodynamics such that a portion of the enthalpic and entropic differences may well be associated with differences in the enthalpy and entropy of the interactions with water.

Nevertheless, these results strongly suggest that the willardiine partial agonists can bind in either the charged or uncharged state of the uracil ring and provide a tool for showing how the enthalpy of binding can be optimized. The differences between the binding of the charged form of the uracil ring and the uncharged form are negligible in the crystal structure. Therefore, the difference is likely to arise, at least in

part, from the increased strength of the H-bonding in the charged form that would stabilize the closed lobe form of the protein. This increases the enthalpy of binding at an entropic cost.

DISCUSSION

A great deal of consideration has been given to strategies for the development of lead compounds for drug development. Although large hydrophobic drugs can be optimized to relatively high free energies of binding, the driving force is often a change in the entropy due to the increase in the degrees of freedom of water when the hydrophobic surface is buried in the protein. This sometimes results in compounds with poor solubility and selectivity. In a number of cases (e.g., HIV protease inhibitors³³ and statins³⁴), optimizing binding enthalpy improved the affinity and selectivity. In the case of glutamate receptors, drugs targeting the agonist-binding site and the several allosteric sites have significant therapeutic potential. Of those drugs that act at the agonist-binding site, subtype selective antagonists may be more likely to have therapeutic efficacy for AMPA and kainate receptors, whereas partial agonists seem to have better therapeutic profiles for NMDA receptors.³⁵ Our studies of willardiine partial agonists suggested that even when bound, the receptor exhibits considerable dynamics on the microsecond to millisecond time scale.³⁶ The electronegativity of the substituent has been correlated with the affinity of the willardiine derivative, and the size of the substituent has been correlated with efficacy.¹⁴ Measurements of HD exchange,³⁷ disulfide trapping experiments,³⁸ and residual dipolar coupling measurements³⁹ suggested that it is the stability of the fully closed lobe form that determines the efficacy of the partial agonist. For the halogenated willardiines, all of the previous studies were conducted below the uracil pK_a , so that the uncharged form predominated, and the binding was driven largely by entropy.¹² While the interaction with lobe 2 is clearly not hydrophobic, in the uncharged state, the H-bonds are not formed through charged interactions and are thus weaker than what one would see with, for example, the γ -carboxyl of glutamate. The work described here suggests that interactions with lobe 2 that are driven by charge lead to higher enthalpies of binding and lower entropy (possibly accompanied by lower dynamics in the ligand–receptor complex). This would suggest that in the future design of partial agonists for NMDA receptors or antagonists for AMPA and kainate receptors, an important consideration would be to build one or more charge interactions into the portion of the molecule that interacts with lobe 2, taking into consideration transfer through the blood–brain barrier in the case of drugs targeted to the CNS. These results illustrate the power of ITC in combination with X-ray crystallography and NMR spectroscopy in improving our understanding of the important thermodynamic characteristics of ligand binding to this essential neurotransmitter receptor.

ASSOCIATED CONTENT

Supporting Information

Thermograms and integrated data for the binding of derivatives not shown in the body of the paper at pH 7.2 and 20 °C (Figure S1) and structural statistics for the crystal structure of the GluA2 LBD bound to nitrowillardiine (NW) at pH 3.5 (Table S1). This material is available free of charge via the Internet at <http://pubs.acs.org>.

AUTHOR INFORMATION

Corresponding Author

*E-mail: reo1@cornell.edu. Telephone: (607) 253-3650. Fax: (607) 253-3659.

Funding

This work was supported by a grant from the National Institutes of Health (R01-GM068935) to R.E.O. This work is based in part upon research conducted at the Cornell High Energy Synchrotron Source (CHESS). CHESS is supported by the National Science Foundation (NSF) and the National Institute of General Medical Sciences (NIGMS) via NSF Grant DMR-0936384, and the MacCHESS resource is supported by NIGMS Grant GM-103485.

Notes

The authors declare no competing financial interest.

ACKNOWLEDGMENTS

We thank J. W. Brady, L. Nowak, C. P. Ptak, B. Romero, and G. A. Weiland (Cornell University) for helpful discussions.

ABBREVIATIONS

AMPA, α -amino-3-hydroxy-5-methyl-4-isoxazole-propionic acid; CIW, (S)-5-chlorowillardiine; GluA2, subtype of the AMPA receptor; ITC, isothermal titration calorimetry; FW, (S)-5-fluorowillardiine; HW, willardiine; IW, (S)-5-iodowillardiine; LBD, ligand-binding domain; NMDA, N-methyl-D-aspartic acid; NW, (S)-5-nitrowillardiine.

REFERENCES

- (1) Freire, E. (2008) Do enthalpy and entropy distinguish first in class from best in class? *Drug Discovery Today* 13, 869–874.
- (2) Freire, E. (2009) A thermodynamic approach to the affinity optimization of drug candidates. *Chem. Biol. Drug Des.* 74, 468–472.
- (3) Ferenczy, G. G., and Keseru, G. M. (2010) Thermodynamics guided lead discovery and optimization. *Drug Discovery Today* 15, 919–932.
- (4) Traynelis, S. F., Wollmuth, L. P., McBain, C. J., Menniti, F. S., Vance, K. M., Ogden, K. K., Hansen, K. B., Yuan, H., Myers, S. J., Dingledine, R., and Sibley, D. (2010) Glutamate receptor ion channels: Structure, regulation, and function. *Pharmacol. Rev.* 62, 405–496.
- (5) Wo, Z. G., and Oswald, R. E. (1995) Unraveling the modular design of glutamate-gated ion channels. *Trends Neurosci.* 18, 161–168.
- (6) Sobolevsky, A. I., Rosconi, M. P., and Gouaux, E. (2009) X-ray structure, symmetry and mechanism of an AMPA-subtype glutamate receptor. *Nature* 462, 745–756.
- (7) Chen, G. Q., and Gouaux, E. (1997) Overexpression of a glutamate receptor (GluR2) ligand binding domain in *Escherichia coli*: Application of a novel protein folding screen. *Proc. Natl. Acad. Sci. U.S.A.* 94, 13431–13436.
- (8) Du, M., Reid, S. A., and Jayaraman, V. (2005) Conformational changes in the ligand binding domain of a functional ionotropic glutamate receptor. *J. Biol. Chem.* 280, 8633–8636.
- (9) Fenwick, M. K., and Oswald, R. E. (2010) On the mechanisms of α -amino-3-hydroxy-5-methylisoxazole-4-propionic acid (AMPA) receptor binding to glutamate and kainate. *J. Biol. Chem.* 285, 12334–12343.
- (10) Jane, D. E., Hoo, K., Kamboj, R., Deverill, M., Bleakman, D., and Mandelzys, A. (1997) Synthesis of willardiine and 6-azawillardiine analogs: Pharmacological characterization on cloned homomeric human AMPA and kainate receptor subtypes. *J. Med. Chem.* 40, 3645–3650.
- (11) Dolman, N. P., More, J. C., Alt, A., Knauss, J. L., Troop, H. M., Bleakman, D., Collingridge, G. L., and Jane, D. E. (2006) Structure-activity relationship studies on N3-substituted willardiine derivatives

acting as AMPA or kainate receptor antagonists. *J. Med. Chem.* 49, 2579–2592.

(12) Ahmed, A., Thompson, M., Fenwick, M., Romero, B., Loh, A., Jane, D., Sondermann, H., and Oswald, R. (2009) Mechanisms of antagonism of the GluR2 AMPA receptor: Structure and dynamics of the complex of two willardiine antagonists with the glutamate binding domain. *Biochemistry* 48, 3894–3903.

(13) Patneau, D. K., Mayer, M. L., Jane, D. E., and Watkins, J. C. (1992) Activation and desensitization of AMPA/kainate receptors by novel derivatives of willardiine. *J. Neurosci.* 12, 595–606.

(14) Jin, R., Banke, T. G., Mayer, M. L., Traynelis, S. F., and Gouaux, E. (2003) Structural basis for partial agonist action at ionotropic glutamate receptors. *Nat. Neurosci.* 6, 803–810.

(15) Chen, G. Q., Sun, Y., Jin, R., and Gouaux, E. (1998) Probing the ligand binding domain of the GluR2 receptor by proteolysis and deletion mutagenesis defines domain boundaries and yields a crystallizable construct. *Protein Sci.* 7, 2623–2630.

(16) Ptak, C. P., Ahmed, A. H., and Oswald, R. E. (2009) Probing the allosteric modulator binding site of GluR2 with thiazide derivatives. *Biochemistry* 48, 8594–8602.

(17) Singh, R., Blattler, W. A., and Collinson, A. R. (1993) An amplified assay for thiols based on reactivation of papain. *Anal. Biochem.* 213, 49–56.

(18) Singh, R., Blattler, W. A., and Collinson, A. R. (1995) Assay for thiols based on reactivation of papain. *Methods Enzymol.* 251, 229–237.

(19) Ptak, C. P., Hsieh, C. L., Weiland, G. A., and Oswald, R. E. (2014) Role of stoichiometry in the dimer-stabilizing effect of AMPA receptor allosteric modulators. *ACS Chem. Biol.* 9, 128–133.

(20) Sun, Y., Olson, R., Horning, M., Armstrong, N., Mayer, M., and Gouaux, E. (2002) Mechanism of glutamate receptor desensitization. *Nature* 417, 245–253.

(21) Sigurskjold, B. W. (2000) Exact analysis of competition ligand binding by displacement isothermal titration calorimetry. *Anal. Biochem.* 277, 260–266.

(22) Madden, D. R., Abele, R., Andersson, A., and Keinanen, K. (2000) Large-scale expression and thermodynamic characterization of a glutamate receptor agonist-binding domain. *Eur. J. Biochem.* 267, 4281–4289.

(23) Ahmed, A. H., Wang, Q., Sondermann, H., and Oswald, R. E. (2009) Structure of the S1S2 glutamate binding domain of GluR3. *Proteins* 75, 628–637.

(24) Armstrong, N., and Gouaux, E. (2000) Mechanisms for activation and antagonism of an AMPA-sensitive glutamate receptor: Crystal structures of the GluR2 ligand binding core. *Neuron* 28, 165–181.

(25) Gill, A., Birdsey-Benson, A., Jones, B. L., Henderson, L. P., and Madden, D. R. (2008) Correlating AMPA receptor activation and cleft closure across subunits: Crystal structures of the GluR4 ligand-binding domain in complex with full and partial agonists. *Biochemistry* 47, 13831–13841.

(26) Otwinowski, Z., and Minor, W. (1997) Processing of X-ray diffraction data collected in oscillation mode. In *Methods in Enzymology, Volume 276, Macromolecular Crystallography, part A* (Carter, C. W., and Sweet, R. M., Eds.) pp 307–326, Academic Press, New York.

(27) Adams, P. D., Grosse-Kunstleve, R. W., Hung, L. W., Ioerger, T. R., McCoy, A. J., Moriarty, N. W., Read, R. J., Sacchettini, J. C., Sauter, N. K., and Terwilliger, T. C. (2002) PHENIX: Building new software for automated crystallographic structure determination. *Acta Crystallogr. D* 58, 1948–1954.

(28) Emsley, P., and Cowtan, K. (2004) Coot: Model-building tools for molecular graphics. *Acta Crystallogr. D* 60, 2126–2132.

(29) Lidak, M. Y., Dipan, I. V., Paégle, R. A., and Stradyn, Y. P. (1972) (Protolysis of some α -amino- β -(1-pyrimidyl)propionic acids and their analogs). *Khimiya Geterotsiklicheskikh Soedinenii* 5, 708–712.

(30) Wempfen, I., and Fox, J. J. (1964) Spectrometric studies of nucleic acid derivatives and related compounds. VI. On the structure

of certain 5- and 6-halogenouracils and -cytosines. *J. Am. Chem. Soc.* 86, 2474–2477.

(31) Jin, R., and Gouaux, E. (2003) Probing the function, conformational plasticity, and dimer-dimer contacts of the GluR2 ligand-binding core: Studies of 5-substituted willardiines and GluR2 S1S2 in the crystal. *Biochemistry* 42, 5201–5213.

(32) Poon, K., Ahmed, A. H., Nowak, L. M., and Oswald, R. E. (2011) Mechanisms of modal activation of GluA3 receptors. *Mol. Pharmacol.* 80, 49–59.

(33) Ohtaka, H., and Freire, E. (2005) Adaptive inhibitors of the HIV-1 protease. *Prog. Biophys. Mol. Biol.* 88, 193–208.

(34) Carbonell, T., and Freire, E. (2005) Binding thermodynamics of statins to HMG-CoA reductase. *Biochemistry* 44, 11741–11748.

(35) Stanton, P. K., Potter, P. E., Aguilar, J., Decandia, M., and Moskal, J. R. (2009) Neuroprotection by a novel NMDAR functional glycine site partial agonist, GLYX-13. *NeuroReport* 20, 1193–1197.

(36) Fenwick, M. K., and Oswald, R. E. (2008) NMR spectroscopy of the ligand-binding core of ionotropic glutamate receptor 2 bound to 5-substituted willardiine partial agonists. *J. Mol. Biol.* 378, 673–685.

(37) Ahmed, A. H., Ptak, C. P., Fenwick, M. K., Hsieh, C. L., Weiland, G. A., and Oswald, R. E. (2013) Dynamics of cleft closure of the GluA2 ligand-binding domain in the presence of full and partial agonists revealed by hydrogen-deuterium exchange. *J. Biol. Chem.* 288, 27658–27666.

(38) Ahmed, A. H., Wang, S., Chuang, H. H., and Oswald, R. E. (2011) Mechanism of AMPA receptor activation by partial agonists: Disulfide trapping of closed lobe conformations. *J. Biol. Chem.* 286, 35257–35266.

(39) Maltsev, A. S., Ahmed, A. H., Fenwick, M. K., Jane, D. E., and Oswald, R. E. (2008) Mechanism of partial agonism at the GluR2 AMPA receptor: Measurements of lobe orientation in solution. *Biochemistry* 47, 10600–10610.